

A Comparison between Digital Filtering Initialization and Nonlinear Normal-Mode Initialization in a Data Assimilation System

XIANG-YU HUANG, ANNETTE CEDERSKOV, AND ERLAND KÄLLÉN

Danish Meteorological Institute, Copenhagen, Denmark

(Manuscript received 8 June 1993, in final form 19 August 1993)

ABSTRACT

The objective of this study is to examine the performance of the adiabatic digital filtering initialization scheme of Lynch and Huang, the diabatic digital filtering initialization scheme of Huang and Lynch, and the diabatic nonlinear normal-mode initialization scheme of Cederskov in a complete data assimilation system. In particular, the authors wish to examine the handling of observations and the changes that the initialization makes to the analysis in an intermittent data assimilation cycle. As a reference the authors use the adiabatic nonlinear normal-mode initialization of Machenhauer, formulated according to Bijlsma and Hafkenscheid, which is the current operational initialization scheme at the Danish Meteorological Institute.

The initialization schemes tested are found to produce a well-balanced model state that is at least as good as that produced by the reference scheme. Furthermore, the changes to the analysis made by the different initialization schemes are similar and the observations are therefore treated similarly with the different schemes. It is thus found that the introduction of a new initialization procedure has no detrimental effect on the data assimilation cycle. On the contrary, the two diabatic schemes reduce the noise level considerably compared to the adiabatic ones albeit at an increased computational cost. Considering the advantages of a diabatic scheme, in particular the future possibility of including cloud properties in the initialization procedure (Huang and Sundqvist), the use of a diabatic scheme seems well justified. The noise reduction is perhaps not the most important aspect as all schemes behave identically in the handling of observations. Instead, the possibility of including satellite-derived cloudiness and precipitation data in the analysis and initialization cycle is a much more important aspect. From this point of view the digital filter has a clear advantage over the normal-mode initialization scheme as all dependent variables of the model are initialized.

1. Introduction

For numerical weather prediction we need two basic ingredients (as first pointed out by Bjerknes 1904). First, we need an initial state of the atmosphere as defined by observations, and second, we require a physical model of the atmosphere that can be integrated forward in time through a numerical procedure. In deriving initial states from a temporally and spatially incomplete observational dataset many weather prediction centers use a technique called "intermittent data assimilation" (see Daley 1991). This is a cyclic procedure where results from short model integrations (typically 6 h) are used as first-guess fields that are merged with the latest observations to form new initial states for the next model integration and so on. The merging of the first-guess field with observations is called the analysis step, and the output of the analysis is in a statistical sense an optimal initial state for the forecast model. In practice it turns out that the analyzed

state will give rise to spurious oscillations in a forecast model and some kind of filtering procedure is required between the analysis and model integration steps. This filtering is commonly known as the initialization step and several initialization methods have been proposed in the history of numerical weather prediction. Currently the most widely used method is the so-called nonlinear normal-mode initialization technique that was first proposed by Machenhauer (1977). A comprehensive review of data assimilation and initialization techniques can be found in Daley (1991).

The initialization step will introduce changes to the analyzed atmospheric fields and in a statistical sense we are degrading the analysis when initialization is performed. We thus have two requirements on an initialization procedure. 1) It should reduce the spurious oscillations in the forecast model, and 2) it should minimize the changes made to the analysis. Most studies of initialization techniques have concentrated on the first of these two conditions, while the second has received less attention. A particular aspect of the second condition is how the forecast quality is affected by different initialization procedures. Relatively small changes in the analysis may lead to a drastically altered forecast even on short time scales in some weather sit-

Corresponding author address: Dr. Xiang-Yu Huang, Danish Meteorological Institute, Lyngbyvej 100, DK-2100 Copenhagen Ø, Denmark.

uations (Källén and Huang 1988). One of the main reasons for including an initialization procedure in an intermittent data assimilation cycle is to increase the quality of the first-guess fields. If spurious oscillations or other forecast errors are present in the first guess, the observations may be handled incorrectly and this will gradually degrade the performance of the data assimilation system.

In this study we will test two basically different initialization techniques: One is based on normal modes, and slow-moving Rossby waves are separated from fast-moving gravity waves through their different vertical structures. The analysis is projected on the slow Rossby modes and the fast-moving gravity modes are adjusted so as to minimize their initial amplitude growth rate. The second technique is based on digital filter theory. Here an uninitialized short forecast, centered around the analysis time, is filtered so that the high-frequency components are removed. The second method does not require any specification of Rossby and gravity mode structures and is thus incapable of dynamically separating the two types of motion. Instead the digital filter acts directly on a time series from a model integration.

Another aspect of initialization techniques is the spinup of diabatic processes (Krishnamurti et al. 1984). In the adiabatic normal-mode initialization technique (ANM) only mass and wind fields are adjusted, and the ANM takes only adiabatic processes into account. The diabatic processes thus have to be initialized, or spun up, during the forecast integration. Extensions of the ANM technique, which includes diabatic processes, have been proposed by Wergen (1988). Another way of including diabatic processes in the initialization is dynamic initialization. This involves an integration of the forecast model with a selectively damping time integration scheme. Mainly high-frequency components are damped and the damping is uniformly introduced on all model variables. An investigation of this technique has recently been undertaken by Fox-Rabinovitz and Gross (1993). A third alternative is the digital filtering technique that was first applied to numerical weather prediction by Lynch and Huang (1992) and later extended to diabatic processes by Huang and Lynch (1993). The digital filter is applied to a time series of model states that is produced through a model integration. The filter is designed to remove high-frequency noise from the time series and a reintroduction of a filtered initial state in the model will give a smooth time evolution of the forecast.

Recently, a version of the diabatic normal-mode initialization technique (DNM) has been tested with the operational forecast model at the Danish Meteorological Institute by Cederskov (1992). This diabatic normal-mode initialization scheme follows Rasch's (1985) version of Machenhauer's (1977) nonlinear normal-mode initialization scheme. The diabatic effects are computed from the model through short time

integrations. All vertical modes of the model are initialized to retain the vertical structure of the diabatic effects. Condensational heating and boundary layers are concentrated in certain vertical intervals and their effects will be smeared out if only a few vertical modes are retained. As the original Machenhauer (1977) scheme will diverge for the higher vertical modes we use the so-called natural frequencies proposed by Rasch (1985). This scheme will converge also for the higher-order vertical modes.

The digital filtering technique can be used both for adiabatic and diabatic initialization. The filter operates on a time series that is produced by adiabatic backward and adiabatic or diabatic forward integrations of the forecast model. The digital time filter removes the high-frequency noise from the time series. A balanced state is obtained through an adjustment of all dependent variables in the numerical model. In this approach, there is no need for simplifying assumptions such as a constant Coriolis parameter, linearization around a basic state, or a rigid-lid upper boundary condition, which are commonly made in the normal-mode approaches. Also the vertical structure of the model is preserved in contrast to the ANM scheme as discussed above.

By using a numerical weather prediction model, it has been shown that both the adiabatic digital filtering initialization (ADF) scheme of Lynch and Huang (1992) and the diabatic digital filtering initialization (DDF) scheme of Huang and Lynch (1993) give results that are at least as good as those of ANM. More organized and synoptically realistic initial pressure tendency fields are obtained after ADF or DDF when compared with ANM, and noise is effectively removed from forecasts. In DDF, all physical processes are included in the diabatic forward integration and the imbalance caused by these processes, for example, spurious precipitation in mountainous areas, is also removed.

However, the changes made by ADF to the analyses are slightly larger than those made by the conventional ANM. This problem is more severe with DDF, which uses a time series not passing exactly through the analysis time. Although the preceding forecasts converge and the differences between forecasts at 24 h are reasonably small, questions still arise about the applicability of ADF and DDF in a complete data assimilation system. For instance, will the changes due to ADF and DDF influence the subsequent analyses? On the other hand, it may be argued that the larger changes found in Huang and Lynch (1993) can be due to an inconsistency between the digital filtering initialization scheme (ADF or DDF) and the previous initialization scheme (ANM) upon which the analysis is based. [The analysis data used in Lynch and Huang (1992) and Huang and Lynch (1993) is from ECMWF.] If this is the case, will both ADF and DDF have a similar initialization increment to ANM after a certain time of

assimilation? (DDF may have a larger initialization increment due to the diabatic processes involved.)

To answer questions of the type posed above we have tested all the new initialization schemes separately in complete data assimilation cycles. The schemes tested are ADF, DDF, and DNM. In particular we wish to examine the handling of observations and the changes that the initialization makes to the analysis in an intermittent data assimilation cycle. As a reference, the present operational ANM scheme (Källberg 1989) is used. We first describe the properties of the forecast model and the analysis scheme; then we give a description of the initialization schemes and finally the inter-comparison is described.

2. The data assimilation and forecast system

The data assimilation and forecast system used in this study is the High-Resolution Limited-Area Model (HIRLAM) system, which is a comprehensive numerical weather prediction system developed in a joint Nordic and Dutch research project. The system is documented in Källberg (1989). Recent developments and upgrading of the system are reported in Gustafsson (1993). Currently the continued HIRLAM project involves the Irish Meteorological Service in addition to the original Nordic and Dutch participants. Only a short description of the HIRLAM system is given here as more details can be found in the references given above. The intermittent data assimilation system of HIRLAM includes objective analysis, initialization, and a 6-h forecast.

a. Objective analysis

The objective analysis scheme is a limited-area version of the European Centre for Medium-Range Weather Forecasts (ECMWF) analysis system; see Lönnberg and Shaw (1987). The analyzed variables are horizontal wind (u , v), geopotential (Φ), relative humidity (RH), and surface pressure (p_s). Three-dimensional multivariate statistical interpolation is used for u , v , Φ , and p_s . Three-dimensional univariate statistical interpolation is used for RH. Analysis is performed at model levels and on a nonstaggered horizontal grid (a staggered grid is used in the model). The first-guess field is the 6-h forecast from the previous data assimilation cycle. The observation window covers a 6-h span around the analysis times (0000, 0600, 1200, and 1800 UTC). A standard observation set is used, including synoptic observations (SYNOP), ship observations (SHIP), drifting buoys (DRIBU), pilot balloons (PILOT), radiosonde data (TEMP), and automatic aircraft data (AIREP).

b. Initialization

Four different initialization schemes are used in this study:

ANM: adiabatic nonlinear normal-mode initialization (Källberg 1989)

DNM: diabatic nonlinear normal-mode initialization (Cederskov 1992)

ADF: adiabatic digital filtering initialization (Lynch and Huang 1992)

DDF: diabatic digital filtering initialization (Huang and Lynch 1993)

A more detailed description of each scheme is given herein.

1) ADIABATIC NONLINEAR NORMAL-MODE INITIALIZATION

The present operational initialization scheme is based on the adiabatic nonlinear normal-mode initialization scheme originally formulated by Machenhauer (1977) and implemented as described by Bijlsma and Hafkenscheid (1986). To compute the normal modes, the model equations are linearized using a basic state that is dry and motionless. The basic state has a constant temperature and a constant pressure in each model level. The basic-state Coriolis parameter is assumed to be constant. The linearization of the scheme uses a discretization on the mass points of the forecast model. The streamfunction and velocity potential are evaluated at these points. The initialization increments are zero at the horizontal boundaries. All the gravity waves for the first four vertical modes are initialized using adiabatic tendencies, and two nonlinear iterations are used.

2) DIABATIC NONLINEAR NORMAL-MODE INITIALIZATION

To include a diabatic forcing in a normal-mode initialization scheme we use a version of the scheme proposed by Rasch (1985) and compute the diabatic effects through short time integrations of the forecast model. The Rasch scheme is necessary to use as we wish to initialize all the vertical modes. In the standard normal-mode initialization scheme due to Machenhauer (1977) initialization of higher-order modes is impossible as the iteration scheme will diverge.

The difference between the standard normal-mode initialization scheme and the ideas proposed by Rasch can be illustrated through the following example.

Assume that we have the following equation for the time derivative of the amplitude of a gravity mode y with frequency σ , and we include the nonlinear and diabatic terms in the function r :

$$\dot{y} = i\sigma y + r(y). \quad (1)$$

The Machenhauer balance condition $\dot{y} = 0$ is fulfilled if $y = -r(y)/i\sigma$. As this is an implicit equation for y we have to solve it iteratively, and Machenhauer proposed the scheme

$$\Delta y^{\gamma+1} = y^{\gamma+1} - y^\gamma = -\frac{y^\gamma}{i\sigma}, \quad (2)$$

where γ is the iteration number. In the scheme proposed by Rasch (1985) we use an empirically determined frequency σ_E instead of the theoretically computed σ . The σ_E is defined

$$i\sigma_E = \frac{\dot{y}^\gamma - y^{\gamma-1}}{y^\gamma - y^{\gamma-1}}, \quad (3)$$

and the iterative scheme now requires y and \dot{y} at two iteration levels. The first iteration is therefore done with the original Machenhauer scheme, while all subsequent iterations are performed with the Rasch scheme. Following Rasch (1985) the first Δy is multiplied by a factor of 0.05 while all subsequent iteration steps are multiplied with a factor 0.5 to improve the convergence. For some modes we obtain very small values of σ_E , which implies unrealistically large changes in the gravity mode amplitudes. To avoid this problem we simply require that [following Rasch (1985)]

$$|\sigma_E| > \frac{|\sigma|}{4}; \quad (4)$$

otherwise, the theoretical frequency σ will be used.

To obtain the diabatic heating, which will be included in the term $r(y)$ in the equations above, we proceed as follows. A short forecast of ten time steps ahead is carried out and the average of the diabatic heating due to large-scale and convective condensation is computed between time steps 3 and 10. This diabatic heating is now inserted in an Euler time step of the model, and the tendencies computed in this time step are used in the first normal-mode iteration step. All physics except the large-scale and convective condensational heating is thus taken from the model in the first Euler time step. All vertical modes and all gravity modes are now initialized using the scheme described above. Before the next iteration a new short forecast is performed to determine a new averaged diabatic heating that will be used in the following iteration step and so on. In total we iterate six times to produce a balanced initial state. The diabatic heating is recomputed for every iterative step of the normal-mode initialization procedure. This differs from the scheme proposed by Wergen (1988), where the diabatic heating is determined by a short forecast from the uninitialized analysis and is held constant throughout the iterative initialization procedure. Furthermore, in Wergen's scheme only the first few vertical modes are initialized while Cederskov (1992) initializes all vertical modes. This is an important aspect of a diabatic initialization scheme as the diabatic effects are typically concentrated in the boundary layer and the vertical layers where we have condensational heating. If only the first few vertical modes are initialized, the diabatic effects will be projected onto vertical structures that cover the entire vertical domain. The influence of a diabatic effect that is concentrated in a thin layer, such as the boundary layer, will thus be small. As the normal

modes are orthogonal, a larger fraction of the diabatic effect will be taken into account as more vertical modes are included. Using only a few vertical modes may thus cause a spinup problem despite the fact that diabatic effects have been included. The diabatic normal-mode initialization scheme studied here will avoid this problem by retaining the full vertical resolution of the model.

3) ADIABATIC DIGITAL FILTERING INITIALIZATION

The implementation and computation of ADF are done as in Lynch and Huang (1992), except for the definition of the digital filter involved. Following Huang and Lynch (1993) we use an optimal filter with a 3-h time span. The performance of this filter is almost equivalent to the original filter of Lynch and Huang (1992), and the optimal filter is more economic as a shorter time span is used (about 50% savings in CPU time). A schematic diagram for ADF is given in Fig. 1a, in which X represents an arbitrary model variable. Two short-range adiabatic integrations are carried out

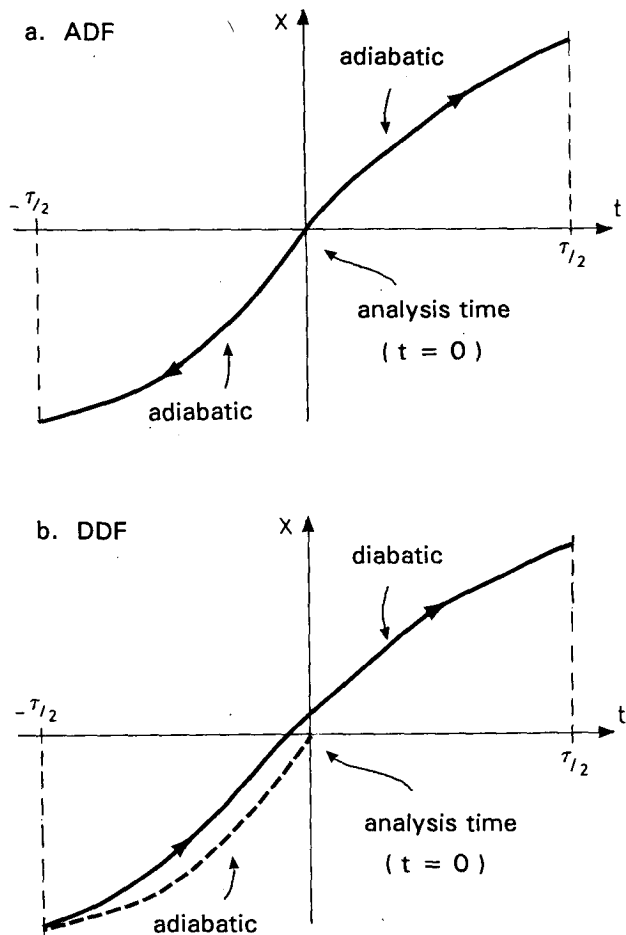


FIG. 1. Schematic diagrams for (a) ADF and (b) DDF.

from the analysis, one backward and one forward in time, each being 1.5 h. As the integrations proceed, all model variables at each model grid point are multiplied by a filter coefficient and accumulated to yield the initialized model state at the end. Formally, the above procedure can be written as

$$X_{\text{ADF}} = \sum_{i=-M}^M F_i X_i^A, \quad (5)$$

where X_{ADF} is the initialized field, F_i is the optimal filter coefficient, i is the time step, M is number of integration steps ($M = 36$ in all the experiments) for half of the filter span, and X_i^A is the time series generated by *adiabatic* integrations. The initialization increments are zero at the boundary. A ten-point relaxation zone, exactly as in the forecast model, is used to guarantee stability in the vicinity of horizontal boundaries.

4) DIABATIC DIGITAL FILTERING INITIALIZATION

To take diabatic processes into account in the filtering of high-frequency noise, the complete model must be used to generate the time series upon which the optimal filter is applied. A schematic diagram for DDF is given in Fig. 1b. As the filter requires the time series to be centered around the analysis time, an integration backward in time for half the filter time span (1.5 h) is needed. The backward integration must be adiabatic due to the irreversibility of diabatic processes. Then a diabatic integration is carried out for 3 h to yield a time series of model states, X_i^D . As the *diabatic* integration proceeds, all model variables are multiplied by the optimal filter coefficient F_i to yield the initialized model state, X_{DDF} :

$$X_{\text{DDF}} = \sum_{i=-M}^M F_i X_i^D. \quad (6)$$

Note that (6) has the same form as (5), the difference being that the time series is produced by a model with all diabatical processes included. The main difficulty with the diabatic scheme is that the backward integration has to be carried out with an adiabatic model in order to center the diabatic integration around the analysis time. As pointed out by Huang and Lynch (1993), there is no guarantee that the diabatic time integration will pass close to the analyzed state at the analysis time. Huang and Lynch (1993) also found that the initialization increments are larger in the diabatic than in the adiabatic case. This, however, did not lead to a degraded forecast in Huang and Lynch (1993), and therefore, the initialization increment was judged to be acceptable. This result was found with a 6-h time span of the filter, and with the 3-h time span used here, the problem should be further reduced.

c. Forecast model

The forecast model is developed from the limited-area version of the ECMWF gridpoint model. It has

undergone extensive changes during the course of the HIRLAM project (Machenhauer 1988; Gustafsson 1993). It is a primitive equation model with u , v , T (temperature), q (specific humidity), and p , as prognostic variables, which are staggered on the Arakawa C grid. It has a rotated latitude–longitude horizontal grid; a hybrid sigma–pressure vertical coordinate; a second-order-accuracy in finite-difference scheme; a leapfrog, semi-implicit scheme with Asselin time filtering. It contains a comprehensive physics parameterization package including a vertical diffusion scheme based on the Monin–Obukov similarity theory in the surface layer and on a Richardson number mixing length formulation in the free atmosphere, a Kuo-type convection scheme, a stratiform condensation scheme, a radiation scheme, and the ECMWF surface parameterization scheme.

The Danish HIRLAM system has been run operationally since 1 January 1991. It has been shown, by both subjective and objective means, to provide a forecast quality that is comparable with other limited-area model systems—for example, the U.K. Meteorological Office Limited-Area Model and the Meteo-France PERIDOT forecasts (Gustafsson 1993). A few additional features are included in the Danish HIRLAM system. To save computer time, physics is computed every third time step. This does not appear to give any problems. Vertical diffusion and shallow convection parameterizations are modified to enhance vertical mixing processes. In the experiments discussed in this study, the time step is 5 min, and 162×136 grid points with a horizontal resolution $0.51^\circ \times 0.51^\circ$ and 16 levels are used. This was the operational setup at the Danish Meteorological Institute until 1 February 1993. Since then, the system is upgraded to have a higher resolution, more horizontal grid points, and more vertical levels. However, the new version has not been used in this study.

3. Results

We have run complete data assimilation cycles for 5 days, from 0000 UTC 13 October 1991 to 1800 UTC 17 October 1991, with different initialization schemes. The experiments will be named after the initialization scheme used—that is, ANM, DNM, ADF, and DDF. The ECMWF analyses are interpreted onto the HIRLAM levels and grids, and used as boundary files. The observation files are also obtained from ECMWF.

a. Reduction of noise

A global measure of the spurious high-frequency noise is the mean absolute tendency of surface pressure, N , defined as

$$N = \frac{1}{J} \sum_{j=1}^J \left| \frac{\partial p_s}{\partial t} \right|_j, \quad (7)$$

where J is the total number of horizontal model grid points. In Fig. 2, N [$\text{hPa} (3 \text{ h})^{-1}$] as a function of time (hours) in the 5-day data assimilation cycle is shown. As a reference, it should be mentioned that N is above $10 \text{ hPa} (3 \text{ h})^{-1}$ if no initialization is performed. The first cycle is expanded and shown on the top of the figure. This cycle has the characteristics of all other cycles. It is clearly shown in Fig. 2 that all three new initialization schemes effectively suppress the high-frequency noise and are somewhat better than ANM in this respect. It is also shown that including the diabatic processes in the initialization lowers the noise level further than if it is excluded.

Another sensitive parameter, which is often used in initialization studies, is the initial pressure tendency. In Fig. 3, the initial surface pressure tendency fields at 0000 UTC 16 October 1991 after ANM, DNM, ADF, and DDF are shown together with the same field from an uninitialized analysis. The unit is the same as N in Fig. 2. The uninitialized run has some extreme values of initial pressure tendency, which are an order of magnitude larger than those from initialized runs. The initialization schemes also give reasonable patterns, compared with the synoptic situation shown in Fig. 4. Most of the initial pressure changes are related to the movement of the weather systems. For instance, the negative tendency between Iceland and the United Kingdom in all initialized runs is a reflection of the eastward movement of the low system over that region. However, small-scale features, most probably noise, can also be identified in Fig. 3. Consistent with the results of Fig. 2, the ANM (Fig. 3a) has a noisier field than DNM (Fig. 3b), ADF (Fig. 3c), and DDF (Fig. 3d). The DDF scheme seems to give the best result in this respect, particularly in mountainous regions such as the Alps. The discretization for both ANM and DNM schemes is not strictly consistent with the staggered C grid used in the model and thus a proper balancing of the smallest scales is not ensured by the normal-mode initialization schemes. This may explain some of the noise left after ANM (Fig. 3a) and DNM (Fig. 3b). Some of the noise may also be due to inconsistencies between the diabatic forecast model and the adiabatic formulation of initialization schemes (Fig. 3a and Fig. 3c). In mountainous regions—for example, in the Alps—the noise that comes from the inadequate handling of orographic effects and related erroneous precipitation processes (can be seen in Figs. 3a–c) is filtered out only by the DDF scheme (Fig. 3d).

b. Precipitation

In Fig. 5, the mean precipitation rate P (mm h^{-1}) is shown as a function of time (h) for all experiments. The small-amplitude oscillations in P are due to the fact that all physical processes are computed only every three time steps and the same tendency from physical processes are kept during the three time steps. Initial

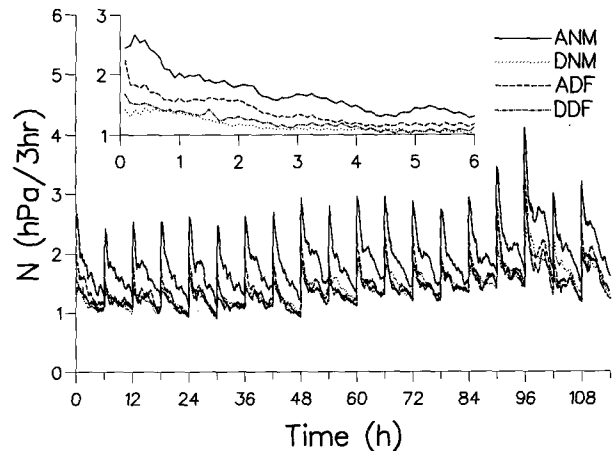


FIG. 2. Mean absolute tendency of surface pressure N [$\text{hPa} (3 \text{ h})^{-1}$] as a function of time (hours) for ANM (full line), DNM (dotted line), ADF (dashed line), and DDF (dot-dash line). The first cycle is expanded and shown on the top of the figure. This cycle has the characteristics of all other cycles.

shocks in precipitation exist in the ANM, DNM, and ADF experiments but not in DDF. These shocks are mainly due to an inconsistency between the humidity treatment in the analysis (e.g., maximum RH is 100%) and that in the model physics (maximum RH is less than 100% when subgrid-scale condensation is considered). Including diabatic processes in the DNM scheme does not overcome this consistency, as the humidity field is not handled by the scheme. It is only in DDF that all model variables are initialized and the initial shocks in precipitation are removed. Sometimes, as in the first cycle, the precipitation is overdamped by the DDF scheme, and this may be related to a spinup problem that is a common feature of many numerical models. We have not investigated this aspect further, but it may be that more insight into the problem could be gained by adjusting some tuning parameters in the precipitation scheme.

We have also compared the model-calculated precipitation rate with precipitation data derived from satellites. An algorithm for calculating precipitation rates from satellite radiances can be found in Karlsson and Liljas (1990), and the data used here has been compiled by K.-G. Karlsson at the Swedish Meteorological and Hydrological Institute. We have data available from 21 time instances during the total assimilation period of 5 days. The data, however, are not covering the whole area of integration, and the different datasets cover different areas within the model domain due to the prevailing satellite orbits. In some situations there is very little precipitation in the satellite data, while in other cases there are well-defined precipitation areas associated with frontal structures. We have not found it meaningful to compute rms scores or some other objective ver-

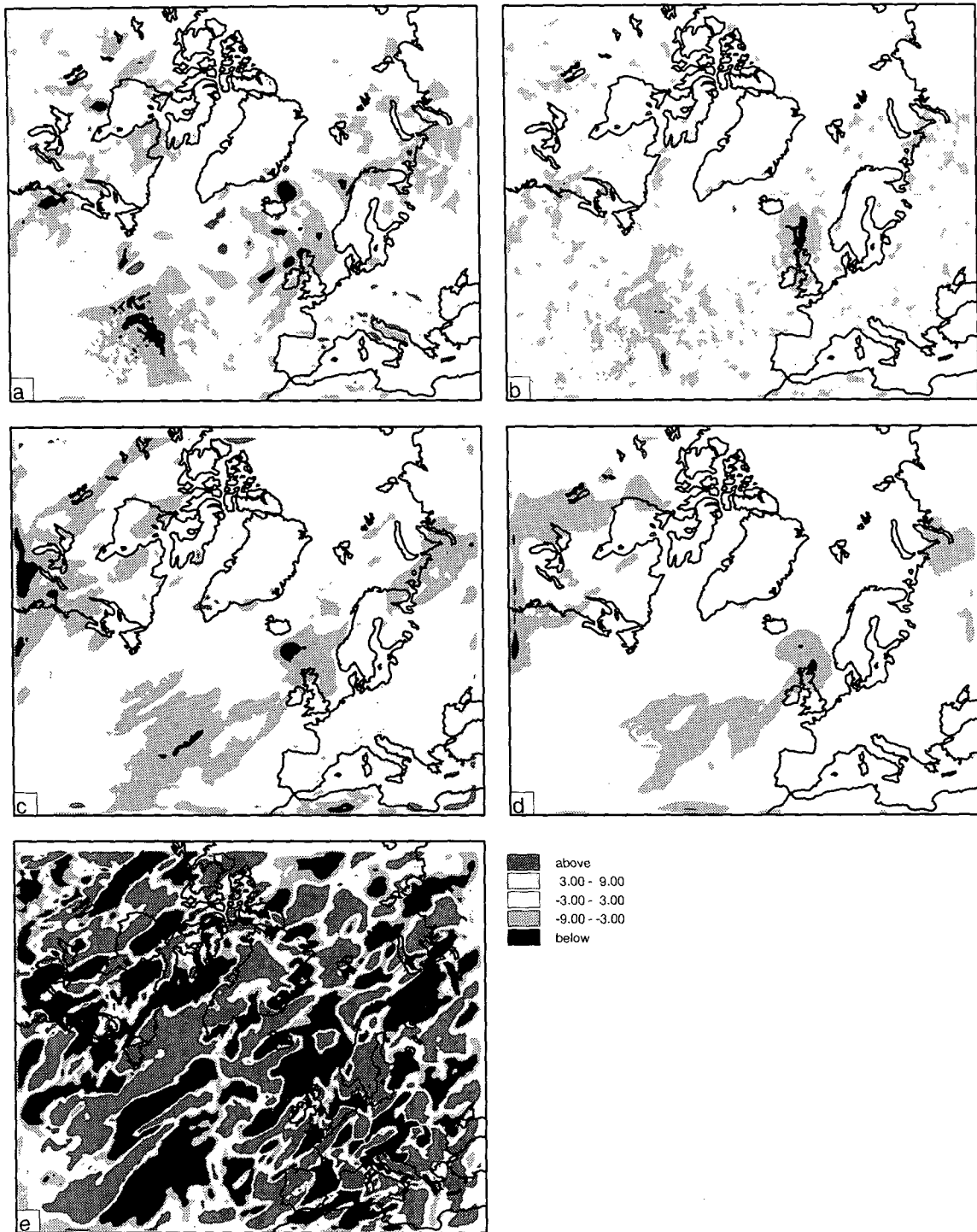


FIG. 3. Initial surface pressure tendency [$\text{hPa} (3 \text{ h})^{-1}$] at 0000 UTC 16 October 1991: (a) after ANM, (b) after DNM, (c) after ADF, (d) after DDF, and (e) without any initialization. The whole integration area is shown and the same gray scale is used.

ification measure for precipitation, as the precipitation data available is incomplete both in time and space. Instead, we choose to show two cases with clear frontal rain areas and compare the model-

calculated precipitation fields with different initializations.

In the first case there is a double precipitation maximum northwest of Scotland that is associated with

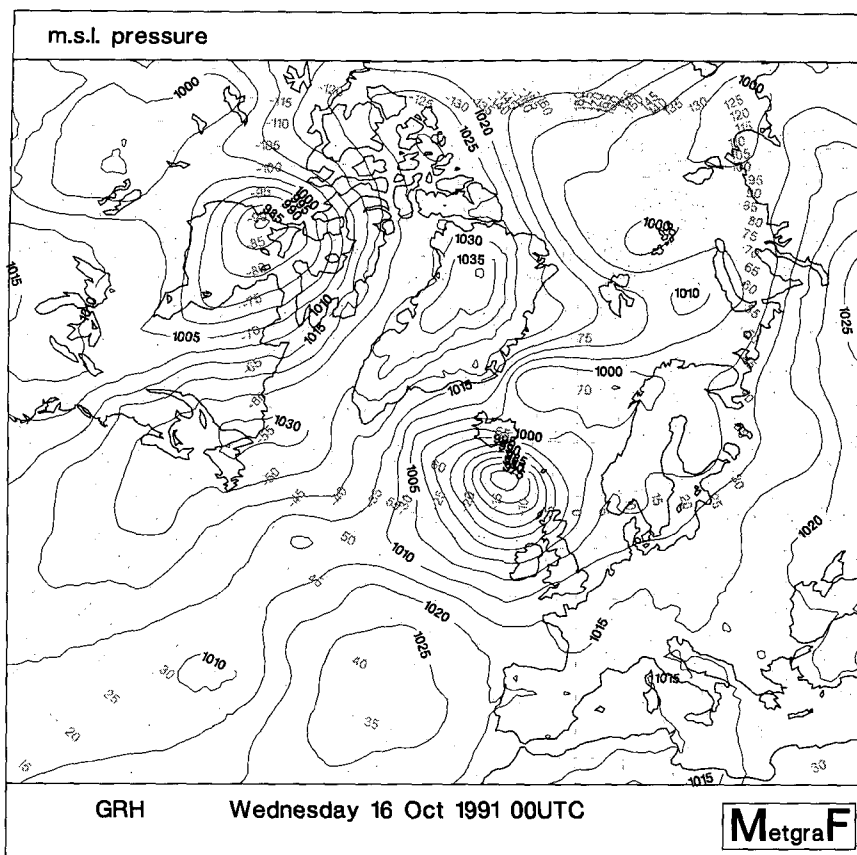


FIG. 4. The mean surface pressure at 0000 UTC 16 October 1991—the same time as in Fig. 3. This is taken from ANM experiment and is very similar to those from other experiments (DNM, ADF, and DDF).

an occluded front (Fig. 6). All four initialization methods produce similar precipitation patterns that have a structure with a single maximum instead of the observed double maximum. The precipitation intensity is too strong compared to observations but the absolute precipitation intensity is the most uncertain aspect of the satellite-derived precipitation data (Karlsson and Liljas 1990). The relative intensity in one situation is more certain and therefore we mainly concentrate on this aspect in our comparison. None of the initialization methods is able to capture the double maximum structure and there is obviously data in the precipitation fields that is not present in other types of observations that have been used in the analysis.

In the second case shown here (Fig. 7) the discrepancy between the observed precipitation pattern and the model-produced fields is even more striking. The forecasts resulting from all initialization methods give precipitation patterns that are weaker and misplaced. In the satellite observations there is a marked frontal feature across the North Sea that is not present in the

model simulations at the correct time. The precipitation rate is quite strong and it is obvious that the forecast would be much improved if the precipitation field somehow could be forced into the analysis. To do this one would have to analyze cloud water and precipitation fields, and to avoid a damping out through an imbalance between the analyzed diabatic forcing and the wind and mass fields, it is necessary to initialize all fields consistently in the model. In addition more experience has to be gained on the accuracy of the satellite-derived precipitation data. Further work is obviously needed to develop such a scheme, and it would be interesting to see whether DDF could handle a situation such as the one presented here.

c. Analysis and initialization errors

To compare the forecast quality and the analysis and initialization errors produced in the experiments with different initialization schemes, the objective verification scheme of Hall (1987) is used, which is based upon the direct relations of the model variables and

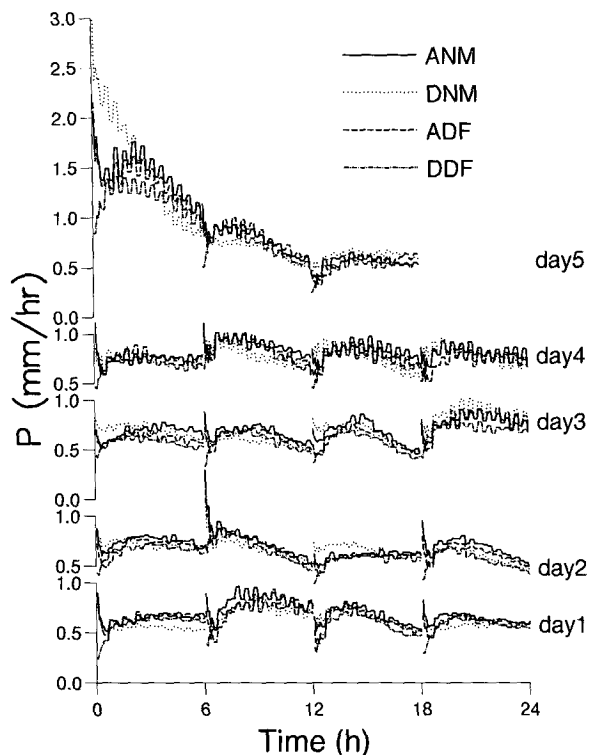


FIG. 5. Mean precipitation rate P (mm h^{-1}) as a function of time (h) for ANM (full line), DNM (dotted line), ADF (dashed line), and DDF (dot-dash line). In this figure, day 1, day 2, day 3, day 4, and day 5 refer to the day in the assimilation cycle.

observations of European radiosonde and synoptic stations, referred to as EWGLAM stations. The stations are unevenly distributed and mainly concentrated in a small part of the model domain for the numerical integrations (European continent). The advantages of the verification scheme include its objective nature and its independence of the initialization schemes used in the data assimilation system.

The bias and rms errors between EWGLAM observations and analysis fields are computed for all the experiments. Most of the conventional parameters, including mean sea level pressure (MSLP), T , u , v , at 850-, 500-, and 250-hPa levels have been examined. Among them, the most sensitive parameter is found to be MSLP, which is shown in Fig. 8. It can be seen that even this most sensitive parameter does not indicate any significant difference between the analysis errors from experiments with different initialization schemes during the 5-day assimilation period.

The bias and rms errors between EWGLAM observations and initialized fields are computed for all the experiments. As an example, the bias and rms in MSLP are shown in Fig. 9. In general it is found that the changes made by initialization schemes lead to a slightly higher error level compared to the analyses. The diabatic schemes produce larger errors than their

adiabatic counterpart. Noticeable differences in the initialization errors are found between experiments with different initialization schemes, especially during the fourth day. While the rms errors are practically the same for all the initialization schemes, it is noted that DNM, ADF, and DDF all give a positive bias and the operational ANM scheme has a near-zero bias. We have no good explanation for this but we note that the bias and rms errors are small. They almost lie within the uncertainty limit of mean sea level pressure when both the observational and typical reduction errors are taken into account (chapter 1 in Daley 1991). Furthermore, comparisons between Fig. 8 and Fig. 9 also point out that the changes introduced by initialization schemes are within an acceptable range and have very little impact on the next analyses. This is also supported by the results on the data handling, which is discussed in the next subsection.

d. First-guess errors and data handling

The main purpose of an initialization procedure is to reduce the noise level in the first-guess field of a data assimilation cycle. The bias and rms in MSLP between EWGLAM observations and first-guess fields are computed and shown in Fig. 10. Consistent with the results of the previous subsection, the errors in the first-guess fields have the same characteristics and are of the same magnitude in all experiments. In other words, all initialization schemes produce first-guess fields of similar quality.

Comparing Fig. 10 with Fig. 8 and Fig. 9, it can also be noticed that the errors in the first-guess fields are larger than those in the analysis and initialization fields. If there is too much noise in the first-guess field, observations may be spuriously rejected in the optimal interpolation scheme (Gustafsson 1981). We thus want to make sure that the different initialization schemes have a similar performance in this respect. This is indeed the case, and in fact the different initialization schemes give exactly the same impact on the observation check in the analysis. Just to give an idea of observation handling in the data assimilation experiments, the number of input observations and the number of rejected TEMP, AIREP, DRIBU, SYNOP, and PILOT observations are shown in Fig. 11. Although Fig. 11 is from the ANM run, the same results hold for DNM, ADF, and DDF runs (but not shown here). The high rejection rates for SYNOPs and DRIBUs are due to some particular properties of the analysis scheme. If observations from the same station occur more than once during one 6-h analysis cycle only the observation closest in time to the central observation time is chosen. All the other observations are discarded. As many DRIBUs are reported every 10 min and some SYNOP stations every 30 min, this leads to very high rejection rates.

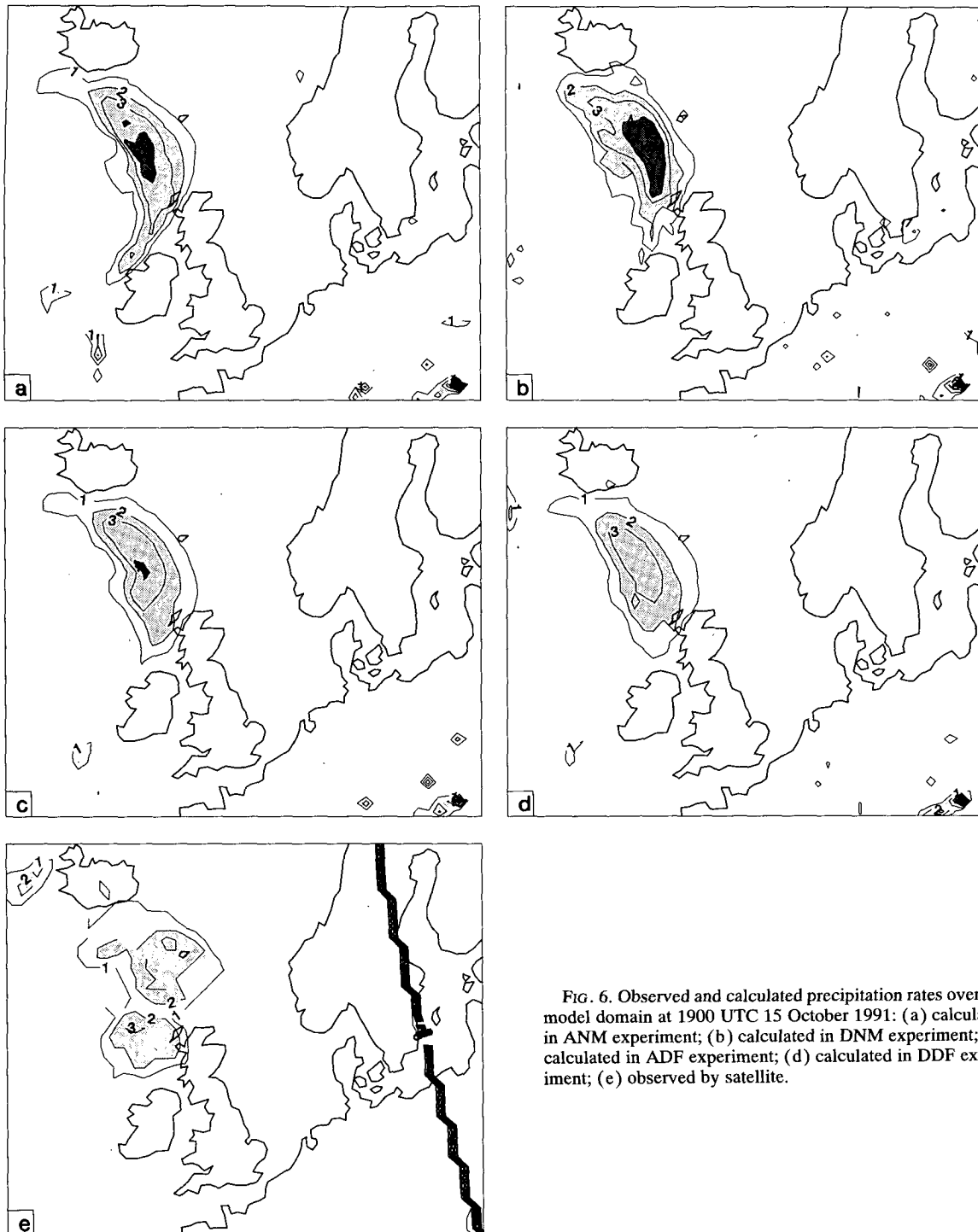


FIG. 6. Observed and calculated precipitation rates over the model domain at 1900 UTC 15 October 1991: (a) calculated in ANM experiment; (b) calculated in DNM experiment; (c) calculated in ADF experiment; (d) calculated in DDF experiment; (e) observed by satellite.

e. Forecast quality

Another very important requirement on an initialization scheme is that the forecast from the initialized field should not be degraded. We have run 36-h fore-

casts from initialized fields at 0000 UTC 13, 14, 15, and 16 October 1991. The bias and rms errors between forecasts and EWGLAM observations are shown in Fig. 12. In most cases (Figs. 12a, 12b, and 12d), ANM,

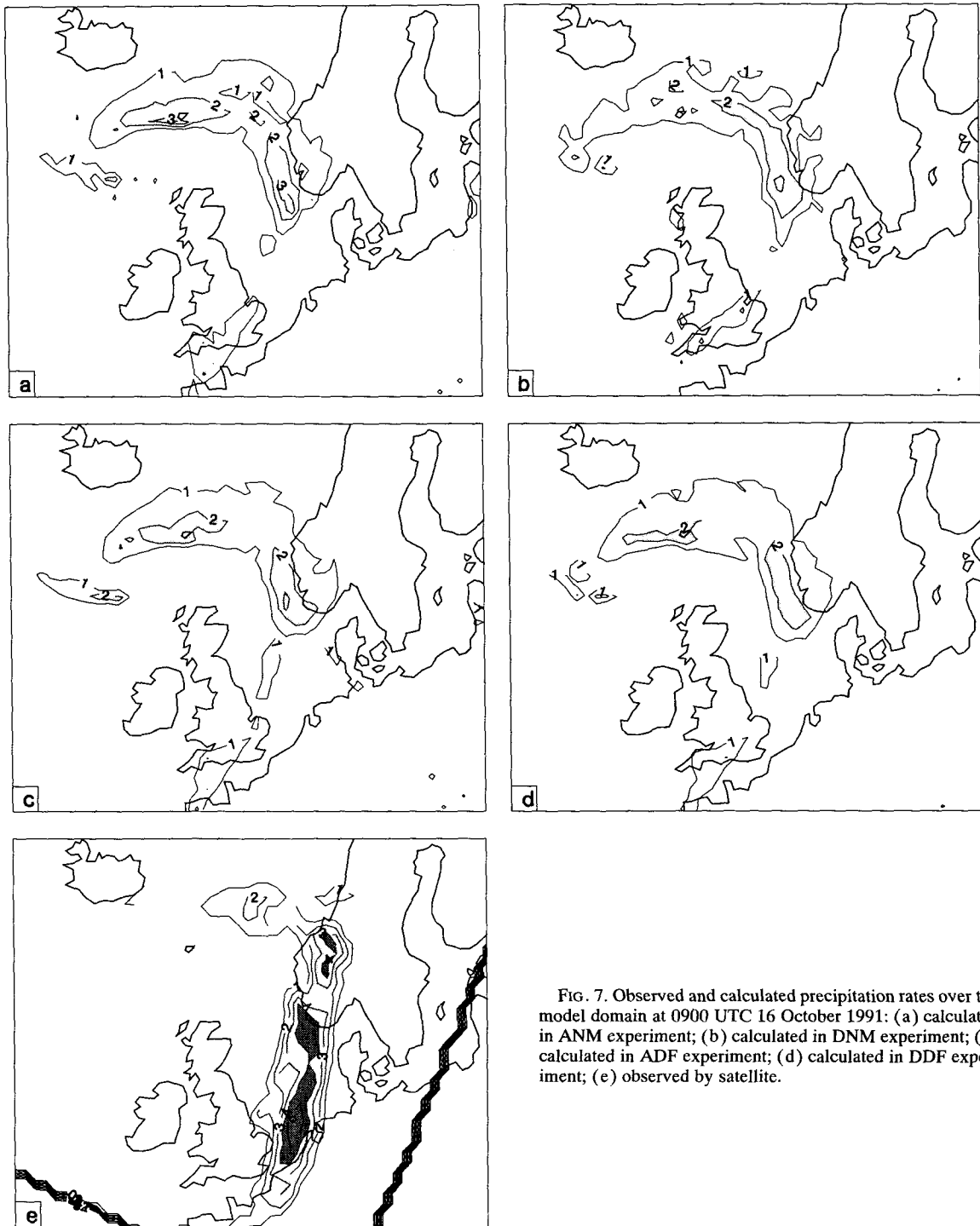


FIG. 7. Observed and calculated precipitation rates over the model domain at 0900 UTC 16 October 1991: (a) calculated in ANM experiment; (b) calculated in DNM experiment; (c) calculated in ADF experiment; (d) calculated in DDF experiment; (e) observed by satellite.

DNM, and ADF give a very similar forecast quality, while DDF gives a clearly different quality—better in Fig. 12a and Fig. 12b and worse in Fig. 12d. It appears that in the DDF forecasts, the MSLP tends to have a

positive bias compared to other forecasts (ANM, DNM, and ADF). Averaged over the four cases (Fig. 12e), there is a small positive bias in the DDF forecast but very little difference in the rms errors. We have

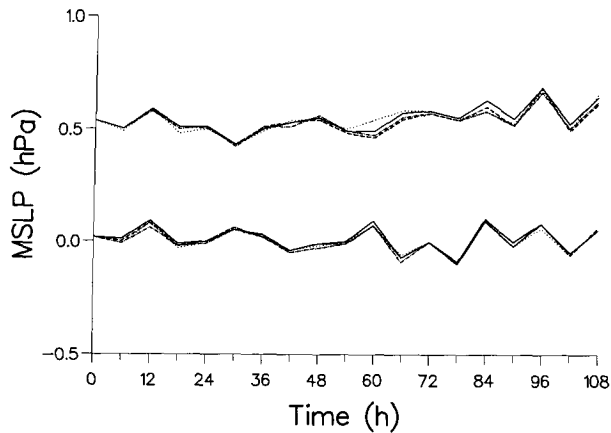


FIG. 8. Observation fitting of mean sea level pressure after analysis for ANM (full line), DNM (dotted line), ADF (dashed line), and DDF (dash-dot line). Both bias (the curves in the lower part of the figure) and rms errors (the curves in the upper part of the figure) are shown.

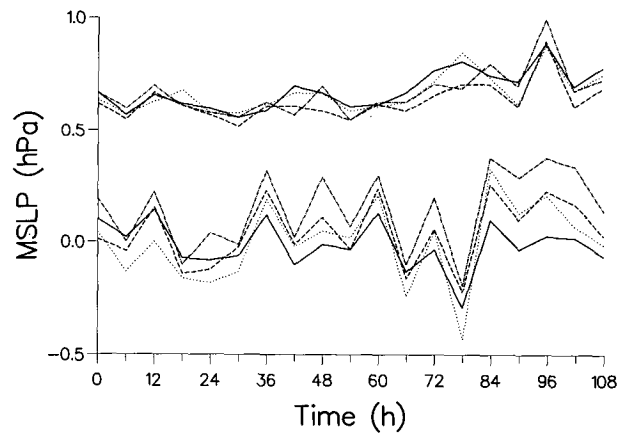


FIG. 9. Observation fitting of mean sea level pressure after initialization for ANM (full line), DNM (dotted line), ADF (dashed line), and DDF (dash-dot line). Both bias (the curves in the lower part of the figure) and rms errors (the curves in the upper part of the figure) are shown.

also examined forecast qualities in other fields; the relative differences due to different initialization schemes are even smaller. Although it has been claimed that forecast skill might be improved through a cumulative effect with an appropriate initialization scheme in a data assimilation system (Fox-Rabinovitz and Gross 1993), we cannot make such a conclusion here as only a few 36-h forecasts are run. On the other hand, the results in Fig. 12 do indicate that the forecasts started from DNM-, ADF-, and DDF-initialized fields are not degraded compared to the operational forecasts that started from ANM-initialized fields.

f. The CPU cost of initialization schemes

The approximate computational cost for the initialization schemes are listed below:

ANM: 100 s
 DNM: 2000 s
 ADF: 225 s
 DDF: 510 s

As a reference, a 6-h forecast takes about 700 s. In ANM, four modes are initialized and two iterations are used. In DNM, all 16 modes are initialized and six iterations are used. For each iteration a 50-min forecast is run to calculate the diabatic effects. In ADF and DDF, the optimal filter is chosen with a 3-h filter span. This means that a 3-h adiabatic integration (1.5 h backward in time and 1.5 h forward in time) of the model is needed for ADF and 1.5-h adiabatic integration (backward in time) and 3-h diabatic integration (forward in time) are needed for DDF. It is possible to reduce the CPU time in the DNM, ADF, and DDF at the cost of letting some more noise develop in the forecast runs.

4. Conclusions

Data assimilation experiments have been carried out to examine the performance of the adiabatic digital filtering initialization scheme of Lynch and Huang (1992), the diabatic digital filtering initialization scheme of Huang and Lynch (1993), and the diabatic nonlinear normal-mode initialization scheme of Cederskov (1992). As a reference we use the adiabatic nonlinear normal-mode initialization of Machenhauer (1977), which is the present operational initialization scheme at the Danish Meteorological Institute.

Compared with the reference initialization scheme, the schemes tested are found to produce a well-balanced model state. The changes to the analysis made

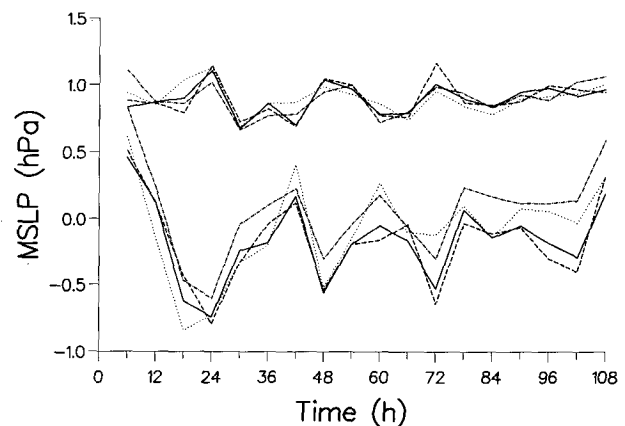


FIG. 10. Observation fitting of mean sea level pressure in the first-guess fields for ANM (full line), DNM (dotted line), ADF (dashed line), and DDF (dash-dot line). Both bias (the curves in the lower part of the figure) and rms errors (the curves in the upper part of the figure) are shown.

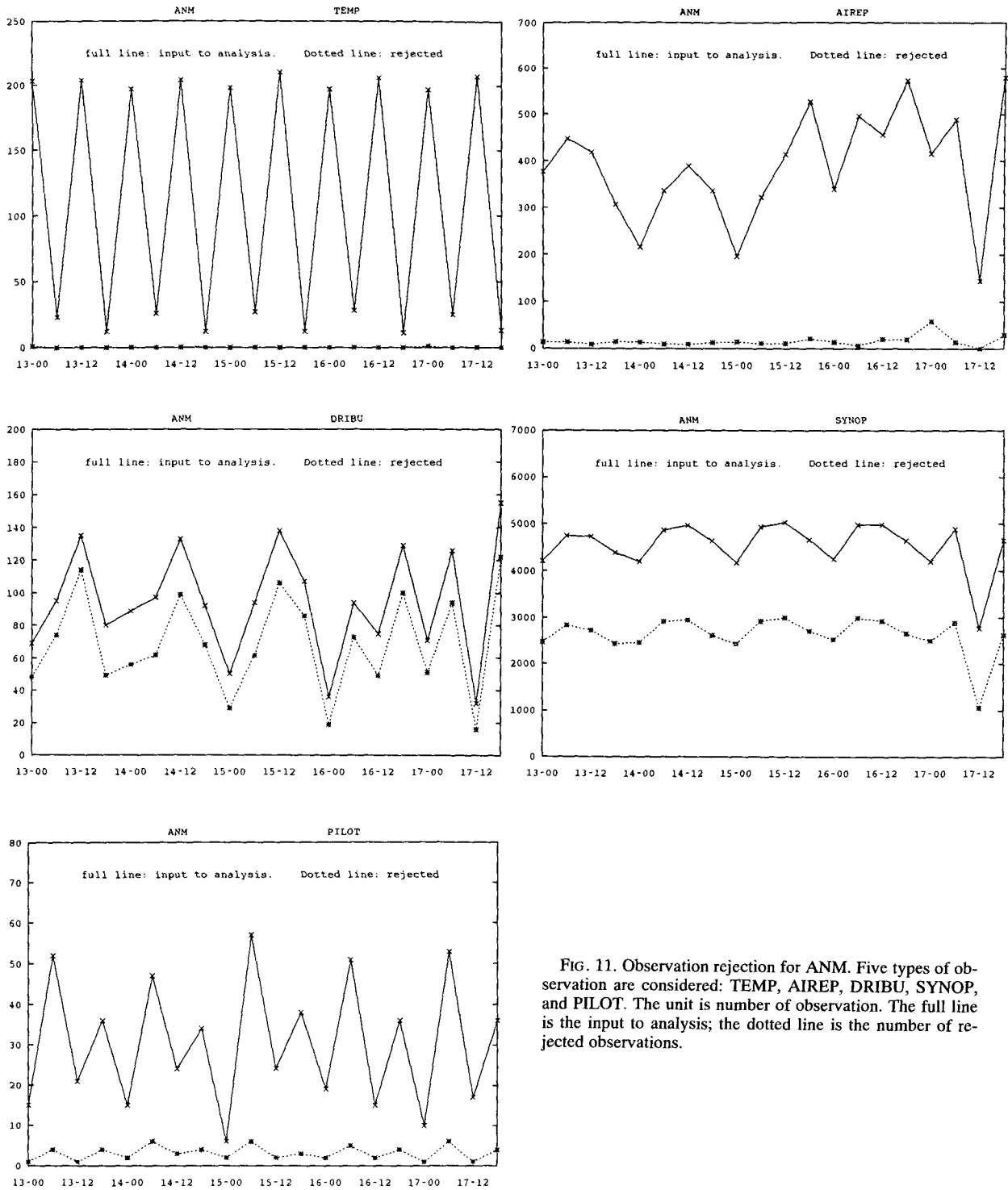


FIG. 11. Observation rejection for ANM. Five types of observation are considered: TEMP, AIREP, DRIBU, SYNOP, and PILOT. The unit is number of observation. The full line is the input to analysis; the dotted line is the number of rejected observations.

by the different initialization schemes are similar and the observations are therefore treated similarly in all data assimilation experiments with the different initialization schemes. Furthermore, the quality of 36-h fore-

casts has not been degraded by the schemes tested. We thus find that the introduction of a new initialization procedure has no detrimental effect on the data assimilation cycle.

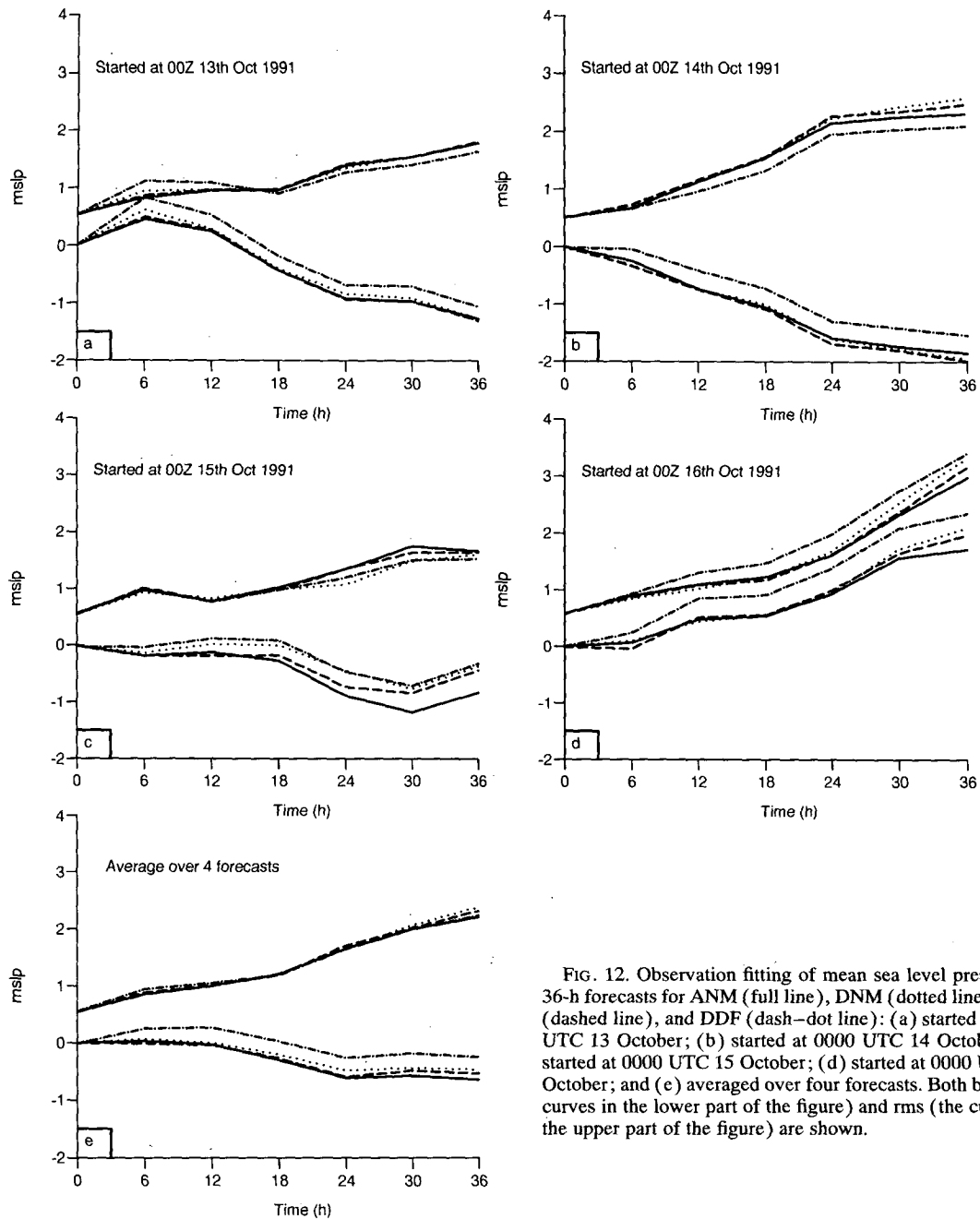


FIG. 12. Observation fitting of mean sea level pressure in 36-h forecasts for ANM (full line), DNM (dotted line), ADF (dashed line), and DDF (dash-dot line): (a) started at 0000 UTC 13 October; (b) started at 0000 UTC 14 October; (c) started at 0000 UTC 15 October; (d) started at 0000 UTC 16 October; and (e) averaged over four forecasts. Both bias (the curves in the lower part of the figure) and rms (the curves in the upper part of the figure) are shown.

The two diabatic schemes reduce the noise level considerably compared to the adiabatic ones albeit at an increased computational cost. The main disadvantage of the diabatic digital filtering initialization is that a backward adiabatic integration is required, which implies that the forward diabatic integration will not pass through the analyzed state around which it is centered. Nevertheless, we feel that the use of a diabatic scheme is well justified considering the advantages of such a

scheme, in particular the future possibility of including cloud properties in the initialization procedure (Huang and Sundqvist 1993). The noise reduction is perhaps not the most important aspect, as all schemes behave identically in the handling of observations. Instead we feel that the possibility of including satellite-derived cloudiness and precipitation data in the analysis and initialization cycle is a much more important aspect. From this point of view the digital filtering initialization

scheme has a clear advantage over the normal-mode initialization scheme, as all dependent variables of the model are initialized.

Acknowledgments. We would like to thank Bernd Kuemmel for assisting us in running the verification package, and Karl-Göran Karlsson for providing us with the satellite data. We are also grateful to Nils Gustafsson, Karl-Göran Karlsson, Peter Lynch, and anonymous reviewers for carefully reading the manuscript and providing us with constructive criticism.

REFERENCES

- Bijlsma, S. J., and L. M. Hafkenscheid, 1986: Initialization of a limited area model: A comparison between the nonlinear normal mode and bounded derivative methods. *Mon. Wea. Rev.*, **114**, 1445–1455.
- Bjerknes, V., 1904: Das Problem von der Wettervorhersage, betrachtet vom standpunkt der Mechanik und der Physik. *Meteor. Z.*, **21**, 1–7.
- Cederskov, A., 1992: Diabatic nonlinear normal mode initialization for a limited area model. Master thesis, Copenhagen University, 72 pp.
- Daley, R., 1991: *Atmospheric Data Analysis*. Cambridge University Press, 457 pp.
- Fox-Rabinovitz, M. S., and B. D. Gross, 1993: Diabatic dynamic initialization. *Mon. Wea. Rev.*, **121**, 549–564.
- Gustafsson, N., 1981: A review of methods for objective analysis. *Dynamic Meteorology; Data Assimilation Methods*, L. Bengtsson, M. Ghil, and E. Källén, Eds., Springer Verlag, 17–76.
- , 1993: HIRLAM 2 final report. HIRLAM Tech. Rep. No. 9, 126 pp. [Available from the Swedish Meteorological and Hydrological Institute, S-60176 Norrköping, Sweden.]
- Hall, C., 1987: A common verification scheme for limited area models. *EWGLAM Newsletter*, **15**, 144–147.
- Huang, X.-Y., and P. Lynch, 1993: Diabatic digital filtering initialization: Application to the HIRLAM model. *Mon. Wea. Rev.*, **121**, 589–603.
- , and H. Sundqvist, 1993: Initialization of cloud water content and cloud cover for numerical prediction models. *Mon. Wea. Rev.*, **121**, 2719–2726.
- Karlsson, K. G., and E. Liljas, 1990: The SMHI model for cloud and precipitation analysis from multispectral AVHRR data. *PROMIS-RAPPORTER 10*, SMHI, Norrköping, Sweden, 74 pp.
- Krishnamurti, T. N., K. Ingles, S. Cocke, T. Kitade, and R. Pasch, 1984: Details of low latitude medium range numerical weather prediction using a global spectral model. Part II: Effects of orography and physical initialization. *J. Meteor. Soc. Japan*, **62**, 613–648.
- Källberg, P., 1989: The HIRLAM level 1 system. Documentation manual, 160 pp. [Available from the Swedish Meteorological and Hydrological Institute, 60176 Norrköping, Sweden.]
- Källén, E., and X.-Y. Huang, 1988: The influence of isolated observations on short-range numerical weather forecasts. *Tellus*, **40A**, 324–336.
- Lönnberg, P., and D. Shaw, 1987: ECMWF Data Assimilation—Scientific Documentation. ECMWF Research Manual 1, 10/87 2nd Revised Edition.
- Lynch, P., and X.-Y. Huang, 1992: Initialization of the HIRLAM model using a digital filter. *Mon. Wea. Rev.*, **120**, 1019–1034.
- Machenhauer, B., 1977: On the dynamics of gravity oscillations in a shallow water model with applications to normal model initialization. *Beitr. Atmos. Phys.*, **50**, 253–271.
- , 1988: HIRLAM final report. HIRLAM Tech. Rep. No. 5, 116 pp. [Available from the Danish Meteorological Institute, DK-2100 Copenhagen, Denmark.]
- Rasch, P. J., 1985: Developments in normal mode initialization. Part 2: A new method and its comparison with currently used schemes. *Mon. Wea. Rev.*, **113**, 1753–1770.
- Wergen, W., 1988: The diabatic ECMWF normal mode initialization scheme. *Beitr. Atmos. Phys.*, **61**, 274–302.